Journal of Information Systems Engineering and Management
2025, 10(4)
e-ISSN: 2468-4376
https://www.jisem-journal.com/

Research Article

One-Dimensional Modeling of a Radiofrequency Discharge in an Electropositive Gas at Low Pressure

Mohamed MARICH[1*], Elhadj HABEL[1]

[1]*Departement of Science and Technology, Faculty of Science and Technology, University Ahmed Benyahia El-Wancharissi of Tissemsilt, Bougara Ben Hamouda road, 38000 Tissemsilt, Algeria;*

**Corresponding author, Mohamed MARICH, Email*: marich.mohamed@univ-tissemsilt.dz

ARTICLEINFO

Received: 20 Dec 2024
Revised: 05 Sept 2025
Accepted: 01 Nov 2025

ABSTRACT

This work presents, through numerical modeling, the fundamental properties of radio frequency electrical discharge type. A one-dimensional (1-D) fluid model, consisting of the first three moments of the Boltzmann equation (equation of continuity, momentum transfer, and electron energy) auto-consistently coupled to the Poisson equation, is used. The discretization of the equations of this model is carried out by the finite difference exponential flux scheme which can take into account the enormous density gradients and inversions of the electric field in the cathode sheath. A study of a radiofrequency discharge is carried out for an electropositive gas (Argon). The 1-D fluid model developed in this study gives a prediction of the electrical characteristics and general properties of radiofrequency electric discharges.

Keywords: Numerical modeling, radiofrequency discharge, Poisson equation, fluid model, electropositive gas.

INTRODUCTION

Various applications of plasma technology have gained tremendous attention in recent years [1]. An electrical discharge heats free electrons, which create reactive plasma species (molecular radicals, ions, and radiation) at endothermic inelastic collisions with the source gas molecules in the gas phase [2]. RF glow discharges are used in a wide variety of applications in modern science and technology [1]. One of the largest and most important fields of application is the microelectronics industry, where RF glow discharges are used for etching of surfaces to form topographical surface features, as well as for depositing thin films. Similarly, glow discharges are used extensively in the materials processing industries for deposition of various thin films, coatings, and surface layers, and may additionally be employed for surface cleaning, pretreatment, and modification processes [3]. RF plasmas are also used in analytical chemistry for qualitative and quantitative elemental diagnostics of materials, primarily through optical and spectral spectroscopy. Ion implantation by immersion remains a widely used method for the production of semiconductor electronic devices and for material strengthening [4]. Modeling and numerical simulation, indispensable complements to experimental analysis, play an important part in the study of plasmas [5]. This work deals with the numerical method for solving the first three moments of the Boltzmann equation in the case of an electropositive radiofrequency discharge. The developed model makes it possible to obtain the spatial variations at different points of the RF cycle and the spatio-temporal distributions of the fundamental parameters of the discharge such as electron density, positive ion density, electric potential, electric field, and electron temperature.

MODEL FORMULATION

The developed model is based on solving the first three moments of the Boltzmann equation. These three moments which are the equations of continuity, momentum transfer, and electron energy. These moments are strongly coupled to the Poisson equation using the local mean energy approximation. In this approximation, it is assumed that all average quantities depend only on the local average energy of the particles. In other words, the distribution function is completely determined by density and local average electron or ion energy (e.g. a Maxwellian distribution). This hypothesis of the average energy can serve as a closure relation for a system of equations that describes the kinetics of charged particles [6].

Journal of Information Systems Engineering and Management
2025, 10(4)
e-ISSN: 2468-4376
https://www.jisem-journal.com/

Research Article

A simple model only contains electrons and positive ions (Argon) in a one-dimensional geometry can then be constituted by system of equations [7]. The equation of continuity and momentum transfer for electrons is given by:

$$\frac{\partial n_e}{\partial t} + \frac{\partial \Phi_e}{\partial x} = R_i \tag{1}$$

$$\Phi_e = -n_e \mu_e E - D_e \frac{\partial n_e}{\partial x} \tag{2}$$

The continuity and momentum transfer equation for positive ions is given by:

$$\frac{\partial n_+}{\partial t} + \frac{\partial \Phi_+}{\partial x} = R_i \tag{3}$$

$$\Phi_+ = +n_+ \mu_+ E - D_+ \frac{\partial n_+}{\partial x} \tag{4}$$

The energy equation and the energy flux for electrons written as:

$$\frac{\partial (n_e \varepsilon_e)}{\partial t} + \frac{\partial q_e}{\partial x} = -e\Phi_e E - \sum_j R_j H_j \tag{5}$$

$$q_e = -\frac{5}{3} n_e D_e \frac{\partial \varepsilon_e}{\partial x} + \frac{5}{2} k T_e \Phi_e \tag{6}$$

Where:

$\varepsilon_e = 3kT_e/2$. T_e is the electron temperature, ε_e is the electron energy, k is the Boltzmann constant, and q_e is the flow of electron energy. The summation figured in the equation (5) is over the reactions involving inelastic electron collisions and H_j is the electron energy loss per collision. This summation included ionization and excitation. These reactions can be represented by the following reactions [7]:

$$Ar + e \rightarrow Ar^+ + 2e \tag{7}$$

$$Ar + e \rightarrow Ar^* + e \tag{8}$$

The corresponding reactions rates were expressed as a function of electron temperature using the following Arrhenius forms [7, 8, 9]:

$$R_i = k_{i0} n_e N \exp(-E_i / kT_e) \tag{9}$$

$$R_{ex} = k_{ex0} n_e N \exp(-E_{ex} / kT_e) \tag{10}$$

The transport equations of charged particles are coupled to the Poisson equation for the electric field:

$$\frac{\partial^2 V}{\partial x^2} = -\frac{e}{\varepsilon_0}(n_+ - n_e) \tag{11}$$

The electric field strength is then found from the partial derivatives of the potential function, and is given by

$$E = -\frac{\partial V}{\partial x} \tag{12}$$

SPATIAL AND TEMPORAL DISCRETIZATION

The numerical scheme adopted in our model is similar to that described by Sharfetter and Gummel in the context of electron transport in semiconductors [10]. The equations are discretized by the finite difference method using an exponential scheme. The integration time step is taken constant. The time discretization of transport equations must be implicitely treated, because according to the Freidrichs-Levy condition stability problems due to explicit treatment

Journal of Information Systems Engineering and Management
2025, 10(4)
e-ISSN: 2468-4376
https://www.jisem-journal.com/

Research Article

require very severe restrictions in the time step. The transport equation is solved in a domain Đ which can be discretized into elementary meshes. Solving the equation for electrons that move from x=0 to x=d. Over the interval $[x_i, x_{i+1}]$, the particle flux, the drift velocity and the diffusion coefficient are assumed to be constant. The system of equations is linearized and implicitly integrated.

The discretization of equation (1) and (3) is written in the form:

$$\frac{n_i^{k+1}-n_i^k}{\Delta t}+\frac{\Phi_{i+1/2}^{k+1}-\Phi_{i-1/2}^{k+1}}{\Delta x}=S_i^k \tag{13}$$

With:

$$\Phi_{i+1/2}^{k+1}=\frac{n_{i+1}^{k+1}D-n_i^{k+1}D\exp(T_1)}{\Delta x}\ \frac{T_1}{1-\exp(T_1)} \tag{14}$$

$$\Phi_{i-1/2}^{k+1}=\frac{n_i^{k+1}D-n_{i-1}^{k+1}D\exp(T_2)}{\Delta x}\ \frac{T_2}{1-\exp(T_2)} \tag{15}$$

$$T_1=-s\frac{\mu}{D}\left(V_{i+1}-V_i\right) \tag{16}$$

$$T_2=-s\frac{\mu}{D}\left(V_i-V_{i-1}\right) \tag{17}$$

Where:

$s=-1$ for electron.

$s=+1$ for positive ion.

n, μ and D are respectively, the density, the flux, the mobility and the diffusion coefficient of the charged particles.

$\Phi_{i+1/2}^{k+1}$ is the flow at the middle point of i and i+1. $\Phi_{i-1/2}^{k+1}$ is the flow at the middle point of i and i-1. S_i^k is the source term at point i evaluated at the moment t_k. Note that, in many works, these source terms are evaluated at time t_k to avoid obtaining highly nonlinear systems.

The transport equation of charged particles, discretized, forms the following system.

$$n_{i-1}^{k+1}\left[\frac{D}{\Delta x^2}\ \frac{T_2\exp(T_2)}{1-\exp(T_2)}\right]+n_i^{k+1}\left[\frac{1}{\Delta t}\ -\frac{D}{\Delta x^2}\left(\frac{T_1\exp(T_1)}{1-\exp(T_1)}+\frac{T_2}{1-\exp(T_2)}\right)\right]+n_{i+1}^{k+1}\left[\frac{D_e}{\Delta x^2}\ \frac{T_1}{1-\exp(T_1)}\right]=S_i^k+\frac{n_i^k}{\Delta t} \tag{18}$$

The discretization of equation (5) is written in the form:

$$\frac{(n_e\varepsilon_e)_i^{k+1}-(n_e\varepsilon_e)_i^k}{\Delta t}+\frac{5}{3}\frac{(\Phi_e)_{i+1/2}^{k+1}-(\Phi_e)_{i-1/2}^{k+1}}{\Delta x}=(S_e)_i^k \tag{19}$$

With:

$$(\Phi_e)_{i+1/2}^{k+1}=\frac{(n_e\varepsilon_e)_{i+1}^{k+1}D_e-(n_e\varepsilon_e)_i^{k+1}D_e\exp(T_1)}{\Delta x}\frac{T_1}{1-\exp(T_1)} \tag{20}$$

$$(\Phi_e)_{i-1/2}^{k+1}=\frac{(n_e\varepsilon_e)_i^{k+1}D_e-(n_e\varepsilon_e)_{i-1}^{k+1}D_e\exp(T_2)}{\Delta x}\frac{T_2}{1-\exp(T_2)} \tag{21}$$

$$T_1=\frac{\mu_e}{D_e}\left(V_{i+1}-V_i\right) \tag{22}$$

Journal of Information Systems Engineering and Management
2025, 10(4)
e-ISSN: 2468-4376
https://www.jisem-journal.com/

Research Article

$$T_2 = \frac{\mu_e}{D_e}\left(V_i - V_{i-1}\right) \tag{23}$$

Finally, we obtain the tridiagonal system of equations:

$$(n_e\varepsilon_e)_{i-1}^{k+1}\left[\frac{5}{3}\frac{D_e}{\Delta x^2}\frac{T_2\exp(T_2)}{1-\exp(T_2)}\right]+(n_e\varepsilon_e)_i^{k+1}\left[\frac{1}{\Delta t}-\frac{5}{3}\frac{D_e}{\Delta x^2}\left(\frac{T_1\exp(T_1)}{1-\exp(T_1)}+\frac{T_2}{1-\exp(T_2)}\right)\right]+(n_e\varepsilon_e)_{i+1}^{k+1}\left[\frac{5}{3}\frac{D_e}{\Delta x^2}\frac{T_1}{1-\exp(T_1)}\right]=(S_e)_i^k+\frac{(n_e\varepsilon_e)_i^k}{\Delta t} \tag{24}$$

The Poisson's equation (13) is most often discretized by using central finite-difference scheme.

$$V_{i-1}^k - 2V_i^k + V_{i+1}^k = \Delta x^2 \frac{e}{\varepsilon_0}\left(n_e - n_+\right) \tag{25}$$

The discretized charged particle transport equations, the discretized electron energy equation, and the discretized Poisson equation form a tridiagonal matrix system. The solution is obtained via Thomas's algorithm [6,10].

To achieve a stationary periodic solution, the calculation must be redone for a large number of cycles, which can range from a few hundred to several thousand cycles, depending on the discharge conditions. At each iteration, the results of the previous cycle are used as the initial solution for the following cycle, and this resolution procedure is repeated until it converges to a final solution, i.e. the steady state of the RF discharge.

BOUNDARY AND INITIAL CONDITIONS

In this model, we consider a parallel-electrode radiofrequency discharge extending from x=0 to x=d Where d is the inter-electrode gap.

At x=0 (the left electrode) [7].

$$\Phi_e = -\gamma\Phi_+ \tag{26}$$

$$\Phi_+ = +n_+\mu_+E \tag{27}$$

$$T_e = T_{ec} \tag{28}$$

$$V(t) = -V_{rf}\sin(2\pi ft) \tag{29}$$

At x=d (the right electrode) [7].

$$\Phi_e = -\gamma\Phi_+ \tag{30}$$

$$\Phi_+ = +n_+\mu_+E \tag{31}$$

$$T_e = T_{ec} \tag{32}$$

$$V(t) = 0 \tag{33}$$

γ is the secondary emission coefficient, V_{rf} is the maximum radiofrequency voltage.

The initial distribution of electron and ion densities is given by the following relation [7]:

$$n_e = n_+ = 10^7 + 10^9\left(1-x/d\right)^2\left(x/d\right)^2 \quad (cm^{-3}) \tag{34}$$

RESULTS AND DISCUSSIONS

A radiofrequency discharge in Argon was studied as an example of an electropositive discharge. The following table gathers all the source data and the transport parameters used in our one-dimensional modeling.

Journal of Information Systems Engineering and Management
2025, 10(4)
e-ISSN: 2468-4376
https://www.jisem-journal.com/

Research Article

Table 1: Transport parameters and operating conditions used in the present simulation [5].

Symbol	Value
$d(cm)$	3.0
$P(Torr)$	1.0
$V_{rf}(V)$	25
$f(MHz)$	10
$T_{gas}(K)$	273
$ND_e(cm.s)^{-1}$	1.7×10^{22}
$ND_+(cm.s)^{-1}$	8.0×10^{17}
$N\mu_e(V.cm.s)^{-1}$	8.5×10^{21}
$N\mu_+(V.cm.s)^{-1}$	3.6×10^{19}
$k_{i0}(cm^3/s)$	1.0×10^{-7}
$E_i(eV)$	17.7
$H_i(eV)$	17.7
$k_{ex0}(cm^3/s)$	5.0×10^{-9}
$E_{ex}(eV)$	11.6
$H_{ex}(eV)$	11.6
γ	0.05
$T_{ec}(eV)$	0.5

Figure 1 and Figure 2 respectively represent the spatial distributions of the electron and positive ion densities at 25% and 75% of the RF cycle. It is noted that the positive ion do not follow the instantaneous variations of the electric field because of their inertia; the variation in the density of positive ion is only a function of the position. On the other hand, electrons instantly follow variations in the electric field because of their mobilities. At 25% of the RF cycle, the left electrode has the role of a cathode. The electrons are repelled towards the plasma, encountering a positive ion charge which increases the electric field near the left electrode, causing the sheath to expand in that region of the discharge. At 75% of the RF cycle, the left electrode acts as an anode. The electrons are attracted to this electrode by covering a positive ion charge. Consequently, the electric field decreases and causes the left sheath to contract. In the plasma region, the electron density is practically equal to that of positive ion which explains the low values of the electric field in the plasma.

Journal of Information Systems Engineering and Management
2025, 10(4)
e-ISSN: 2468-4376
https://www.jisem-journal.com/

Research Article

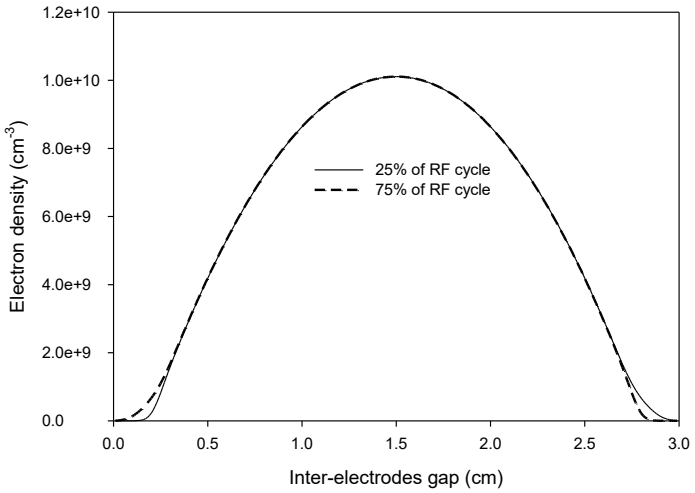

Figure 1: One-dimensional distribution of electron density at 25% and 75% of the RF cycle.

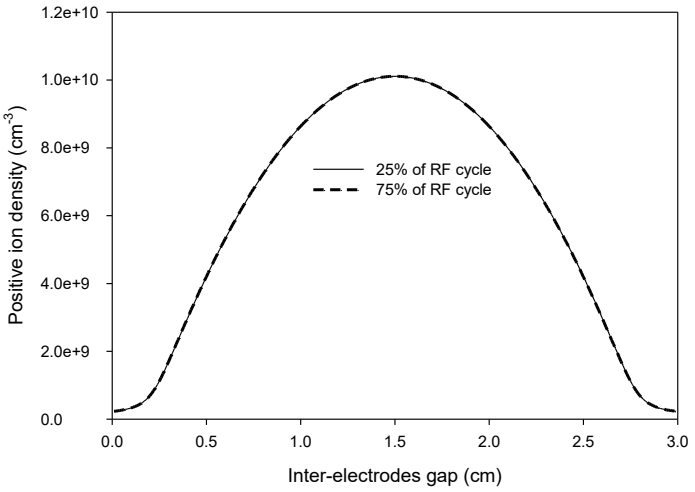

Figure 2: One-dimensional distribution of positive ion density at 25% and 75% of the RF cycle.

The spatial distribution of the electric field and potential at 25% and 75% of the RF cycle is shown in Figure 3 and Figure 4 respectively. We observe that at 25% of the RF cycle, the left sheath undergoes an expansion (increase in sheath thickness and electric field amplitude) and the right sheath undergoes a contraction (decrease in sheath thickness and field amplitude). At 75% of the RF cycle, the situation is quite the opposite, the left sheath is in a state of contraction and the right sheath is in a state of expansion. This phenomenon of sheath contraction and expansion, which repeats at each radio frequency half-cycle, is linked to the kinetics of charged particles (electrons, positive ions). The variation of the electric field in the plasma region is independent of the frequency of variation of the applied potential. The electric field in this area is almost zero because of the net space charge density which tends towards zero in the positive column of the RF discharge.

Journal of Information Systems Engineering and Management
2025, 10(4)
e-ISSN: 2468-4376
https://www.jisem-journal.com/

Research Article

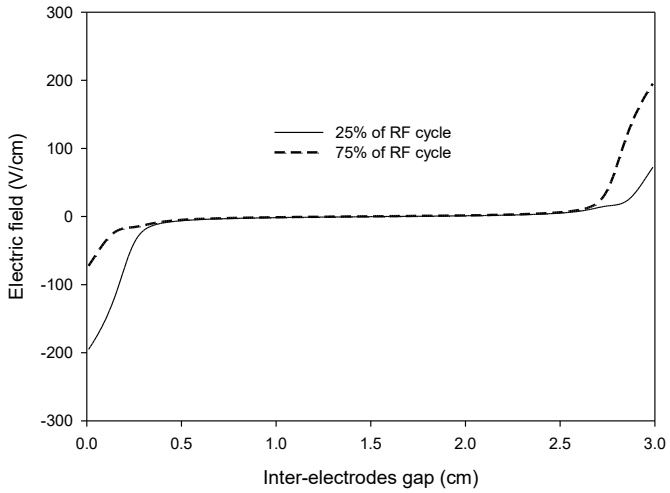

Figure 3: One-dimensional distribution of electric field at 25% and 75% of the RF cycle.

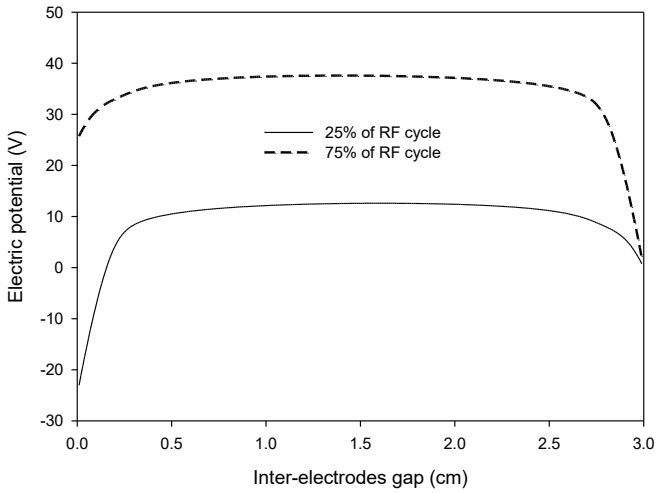

Figure 4: One-dimensional distribution of electric potential at 25% and 75% of the RF cycle.

Figure 5 shows the electron temperature spatial distribution at 25% and 75% of the RF cycle. This figure clearly shows the presence of a cathodic sheath at each half-cycle RF. The electronic temperature gets a maximum in this region of the RF discharge. We know that in the cathode region the electric field is relatively high, which leads to a rapid movement of electrons towards the plasma region. This migration of these particles in the presence of an electric field will generate relatively energetic electrons in this area of discharge. In the plasma region, electrons will lose the energy they gained in the cathode cladding by undergoing inelastic endothermic collisions with the gas neutrals, such as ionization. This is why the electrons cool down in the plasma region and in the anodic sheath.

Journal of Information Systems Engineering and Management
2025, 10(4)
e-ISSN: 2468-4376
https://www.jisem-journal.com/

Research Article

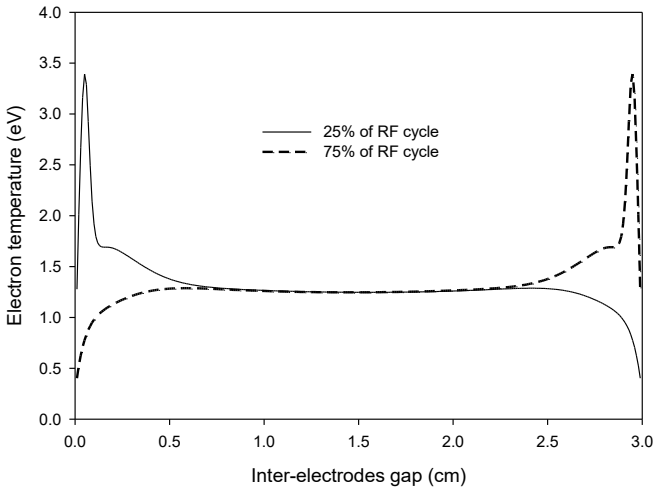

Figure 5: One-dimensional distribution of electron temperature at 25% and 75% of the RF cycle.

Figure 6 and Figure 7 represent the spatio-temporal distributions of electron and positive ion densities. The spatio-temporal distributions of the electric field and the potential are shown respectively in Figure 8 and Figure 9. Figure 10 shows the spatio-temporal distribution of the electron temperature.

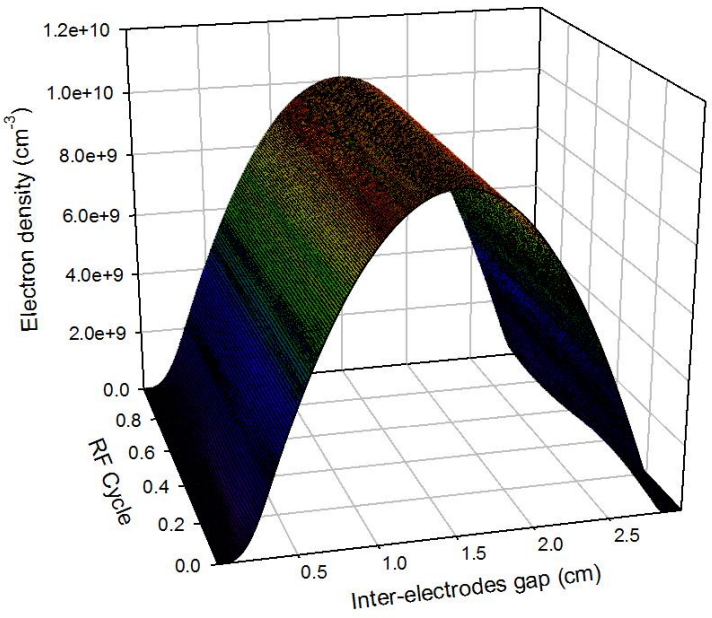

Figure 6: Spatio-temporal distribution of electron density.

Journal of Information Systems Engineering and Management
2025, 10(4)
e-ISSN: 2468-4376
https://www.jisem-journal.com/

Research Article

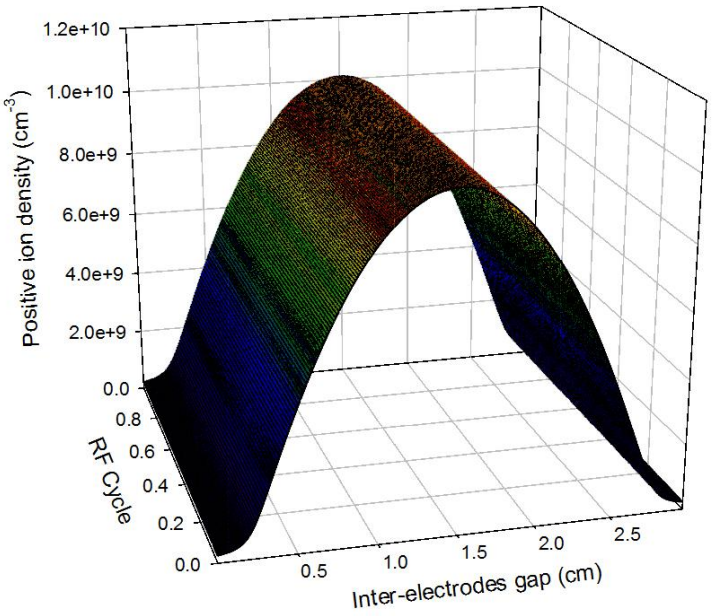

Figure 7: Spatio-temporal distribution of positive ion density.

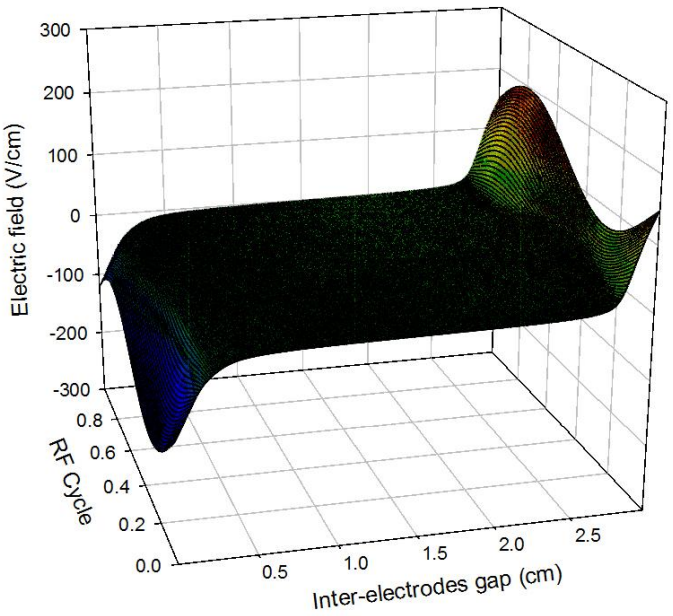

Figure 8: Spatio-temporal distribution of electric field.

Journal of Information Systems Engineering and Management
2025, 10(4)
e-ISSN: 2468-4376
https://www.jisem-journal.com/

Research Article

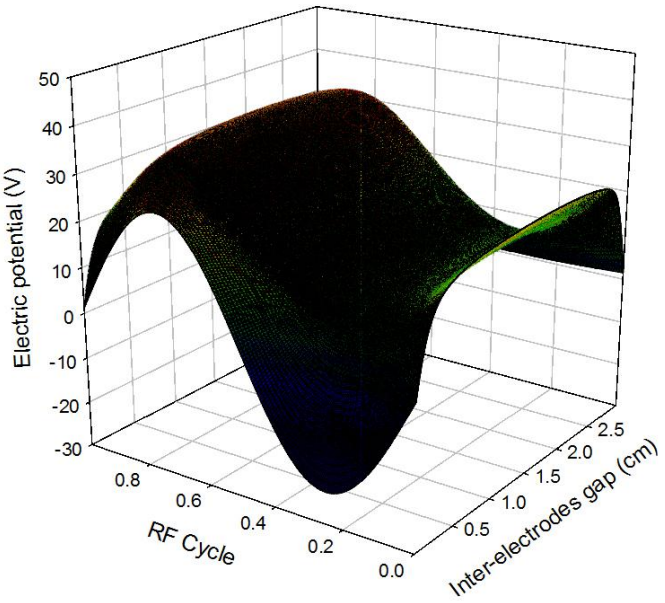

Figure 9: Spatio-temporal distribution of electric potential.

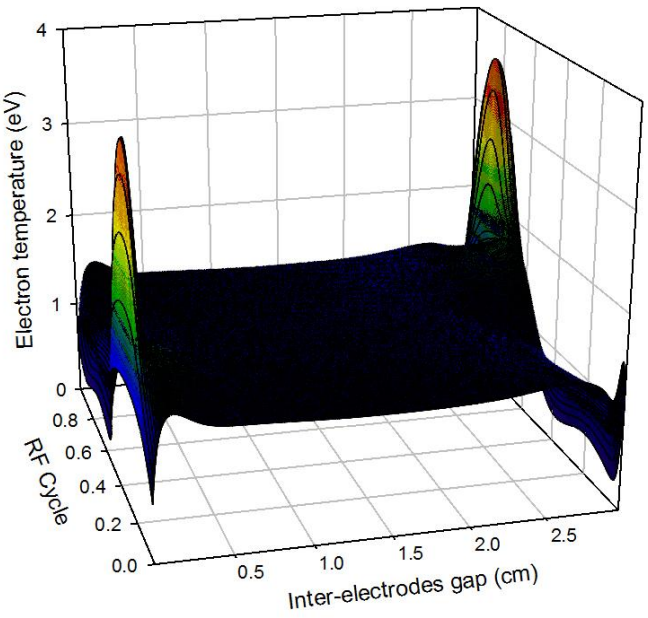

Figure 10: Spatio-temporal distribution of electron temperature.

Journal of Information Systems Engineering and Management
2025, 10(4)
e-ISSN: 2468-4376
https://www.jisem-journal.com/

Research Article

CONCLUSION

The main contribution of this paper is the development of a one-dimensional geometry numerical model. This model predicts the electrical and physical properties of low-pressure radiofrequency discharges in the case of an electropositive gas (Argon). This modeling then appears as a powerful analytical tool that can leads to a better understanding of discharges and to the optimization of plasma reactors. As a future work, one can develop a model in the case of an electronegative gas in multidimensional geometries.

NOMENCLATURE

n_e, n_+	Electron and positive ion density
Φ_e, Φ_+	Electron and positive ion flux
V	Electric potential
E	Electric field
ε_e	Electron energy
T_e	Electron temperature
μ_e, μ_+	Electron and positive ion mobility
D_e, D_+	Electron and positive diffusivity
R_i	Ionization rate
S	Source term for electron and positive ion
S_e	Source term energy
γ	Coefficient for secondary electron emission
N	Neutral species density
e	Elementary charge
ε_0	Free space permittivity
d	Inter-electrode gap
Δx	Spatial step
Δt	Temporal step
T	Period

REFERENCES

[1] E. Poorreza, N. Dadashzadeh Gargari, Modeling and Simulation of a Microwave-Assisted Plasma with Different Input Power for Plasma-Based Applications, Russian Journal of Physical Chemistry, ISSN 1990-7931, (2023).

[2] Miran Mozetič, Low-pressure non-equilibrium plasma technologies: scientifc background and technological challenges, Reviews of Modern Plasma Physics, EISSN 23673192, (2025).

[3] E. Habel, B. Kraloua, A. Hennad, Two-dimensional modeling RF glow discharge at low pressure, PRZEGLĄD ELEKTROTECHNICZNY, ISSN 0033-2097, R. 93 NR 5 (2017).

[4] L. Therese, Radiofrequency plasmas for materials analysis: Experimental, analytical and numerical studies, Doctoral thesis, Paule Sabatier University of Toulouse, (2005).

[5] P. Belengueur, Modeling of radiofrequency discharges in collisional regime, Doctoral thesis, Nancy1 University, nº: 831 (1990).

[6] E. Habel, Two-dimensional modeling of low-pressure radiofrequency discharges, Doctoral thesis, University of Science and Technology of Oran, (2018).

Research Article

[7] S. park and J. Economou, Analysis of low pressure rf glow discharges using a continuum model, J. Appl. Phys. 68, 3904 (1990).

[8] H. Tebani, A. Hennad, three-dimensional modelling of the DC glow discharge using the second order fluid model, PRZEGLĄD ELEKTROTECHNICZNY, ISSN 0033-2097, R.89 NR 8 (2013).

[9] M.H. Elghazaly, S. Solyman, Electron impact ionization and excitation rate coefficients in the negative glow region of a glow discharge, journal of Quantitative Spectroscopy & radiative Transfert 103 (2007), 260-271.

[10] D. L. Scharfetter and H. K. Gummel, Large-signal analysis of a silicon Read diode oscillator, IEEE Trans. Electron Devices ED-16, 64 (1969).